ChemComm

COMMUNICATION

View Article Online
View Journal | View Issue

Cite this: *Chem. Commun.*, 2015, 51, 11401

Received 26th May 2015,
Accepted 10th June 2015

DOI: 10.1039/c5cc04326c

www.rsc.org/chemcomm

Copper(I) complexes as alternatives to iridium(III) complexes for highly efficient oxygen sensing†

Santiago Medina-Rodríguez,[ab] Francisco J. Orriach-Fernández,[b] Christopher Poole,[c] Prashant Kumar,[c] Ángel de la Torre-Vega,*[a] Jorge F. Fernández-Sánchez,*[b] Etienne Baranoff*[c] and Alberto Fernández-Gutiérrez[b]

The complex [Cu(xantphos)(dmp)][PF_6] (dmp = 2,9-dimethyl-1,10-phenanthroline) in a nanostructured metal oxyde matrix shows better sensitivity to oxygen (K_{SV} = 9.74 ± 0.87 kPa^{-1} between 0 and 1 kPa pO_2 and 5.59 ± 0.15 kPa^{-1} between 0 and 10 kPa pO_2) than cyclometallated iridium complexes in the same conditions.

Photoactive complexes based on earth-abundant copper are increasingly studied as alternatives to platinoid metal-based complexes. This is because Cu(I) complexes have attractive photophysical properties[1] (*e.g.* possibly highly emissive metal-to-ligand-charge-transfer (MLCT) state, long luminescence lifetimes, large Stokes shift) whilst copper is much more abundant and low-cost than platinoid metals. For example, Cu(I) complexes have been explored to replace ruthenium(II) complexes as sensitizers for dye-sensitized solar cells (DSSCs)[2] and platinum(II) and iridium(III) as phosphorescent emitters for organic light-emitting diodes (OLEDs)[3] and light-emitting electrochemical cells (LEECs).[4]

Optical oxygen sensing is another key technologic area using phosphorescent noble-metal complexes as champion materials. In this case, the emissive triplet state of the dye is quenched by the oxygen, which has a triplet ground state. In practice, the emission intensity of the dye diminishes as the concentration of oxygen increases. The best reported dyes to date (Table 1) are Pt/PdTFPP (platinum(II)/palladium(II) meso-tetrakis(pentafluorophenyl) porphyrin)[5,6] and N969,[5] a cationic cyclometallated iridium complex. Although Pt/PdTFPP are much better performing than iridium complexes, an important advantage of the latter is the possibility to vary the emission colour over the entire visible spectrum. In this context, Cu(I) complexes are very attractive for sensing of oxygen. However, only few oxygen sensors based on Cu(I) complexes have been reported to date and all display much lower performance than sensors based on platinoid-group metal complexes.[8–14]

Table 1 Comparison of the sensitivity of the O_2 sensing films under study with Pt(II), Pd(II), Ru(II), and Ir(III) sensing films from the literature[a]

Complex	Support	Sensitivity K_{SV} (kPa^{-1})	Sensitivity $\Delta\tau_{0.05}$ (%)	Reference
PtTFPP	AP200/19	25.68[b]	62.53	5
	PS	0.4142[b]	—	5
	Silica beads-silicone	4.23[c]	—	6
PdTFPP	Silica beads-silicone	67.10[d]	—	6
N969	AP200/19	4.79[b]	20.98	5
N1008	AP200/19	1.45[b]	4.44	5
EB146	AP200/19	1.70[b]	9.43	5
ETH^T-3003	AP200/19	0.711[b]	—	7
1	AP200/19	5.59[b]	33.55	This work
	AP200/19	9.74[c]	—	This work
	PS	0.28[b]	1.50	This work
2	AP200/19	5.13[b]	—	This work
	PS	1.59[b]	—	This work
3	PS	2.57[b]	—	This work

[a] Structure of complexes from literature are shown in Fig. S1 (ESI). [b] pO_2 between 0–10 kPa. [c] pO_2 between 0–1 kPa. [d] pO_2 between 0–0.1 kPa.

Smith *et al.* used crystals of $Cu(P^P)(N^N)^+$ complexes (P^P = bis[2-(diphenylphosphino)phenyl]ether (POP) or 4,5-bis-(diphenyl phosphino)-9,9-dimethylxanthene (xantphos) and N^N = 2,9-dimethyl-1,10-phenanthroline (dmp) or 2,9-diisopropyl-1,10-phenanthroline (dipp)) that resulted in very low sensitivity (Stern–Volmer constant K_{SV} between 0.002 and 0.058 kPa^{-1}).[10,12] Wang *et al.* developed an optical sensing layer based on [Cu(POP)(phencarz)](BF_4)-PS (PS = polystyrene; phencarz = 2-(9-ethyl-9*H*-carbaol-2-yl)-1*H*-imidazo[4,5-*f*]-1,10-phenanthroline) showing K_{SV} = 0.39 kPa^{-1}.[11] Shi *et al.* used MCM-41, a mesoporous material, as solid support for [Cu(POP)(PTZ)](BF_4) (PTZ = 5-(2-pyridyl)tetrazole) and achieved the best copper complex-based oxygen sensing film reported so far in the literature with sensitivity to oxygen K_{SV} = 0.50 kPa^{-1}.[9]

Herein we investigate three Cu(I) complexes, [Cu(xantphos)(dmp)][PF_6] (**1**), [Cu(xantphos)(pzpy)][PF_6] (**2**), and [Cu(xantphos)$_2$]

[a] *Department of Signal Theory, Networking and Communications, CITIC-UGR, University of Granada, C/ Periodista Rafael Gómez 2, E-18071 Granada, Spain. E-mail: atv@ugr.es*
[b] *Department of Analytical Chemistry, Faculty of Sciences, University of Granada, Avda. Fuentenueva s/n, E-18071 Granada, Spain. E-mail: jffernan@ugr.es*
[c] *School of Chemistry, University of Birmingham, Edgbaston, B15 2TT, England, UK. E-mail: e.baranoff@bham.ac.uk*

† Electronic supplementary information (ESI) available: Additional figures and description of experimental set-up and methods. See DOI: 10.1039/c5cc04326c

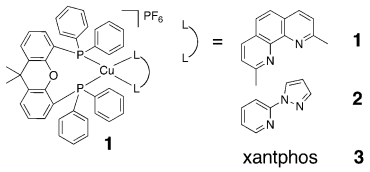

Fig. 1 Chemical structure of the Cu(I) complexes used in this work.

$[PF_6]$ (**3**) (dmp = 2,9-dimethyl-1,10-phenanthroline; pzpy = 2-(1*H*-pyrazol-1-yl)pyridine) (Fig. 1) to develop oxygen-sensitive sensing films with ten times better sensitivity than previously reported copper-based systems. Importantly, we also demonstrate for the first time that these emitters based on earth abundant metals can compete with expensive alternatives such as iridium complexes.

Xantphos is more rigid than POP and so was chosen to limit scrambling of ligands.[15] The complexes were prepared as described in the literature.[16] Sensing films were prepared by dissolving the dyes in chloroform and spincoating the solution on AP200/19 nanostructured films or adding polystyrene (PS) and spincoating the solution on glass (see ESI† for details). As such we obtain six different films named **X**-AP200/19 and **X**-PS (**X** = **1**, **2**, **3**).

Compared to other organometallic compounds used in the development of oxygen-sensitive films, the quantum yields of these Cu(I)-based films are quite low, $\Phi \approx$ 0.1 to 0.3 (Table S1, ESI†), and future efforts should aim at increasing the brightness of these dyes. When exposed to oxygen, the luminescence of the films is completely quenched (Fig. 2 for **1**; Fig. S2 and S3, ESI† for **2** and **3**) but for **3**-AP200/19, in which case the intensity decreased only by half (Fig. S3b, ESI†).‡

The films were characterized first by intensity measurements following the procedure described in ESI.† The variations of the luminescence intensity with the oxygen concentration as well as the Stern–Volmer plots are shown in Fig. 3 and Fig. S4 (ESI†) for

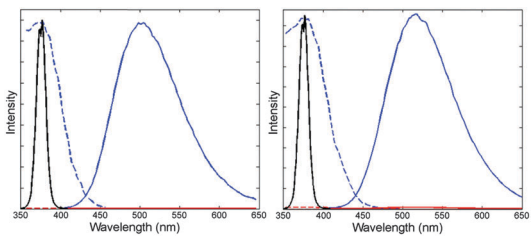

Fig. 2 Excitation (---) and emission (—) spectra of **1**-PS (left) and **1**-AP200/19 (right) in the presence (red) and absence (blue) of oxygen. The black line is the emission spectrum of the LED (λ_{peak} = 375 nm) used

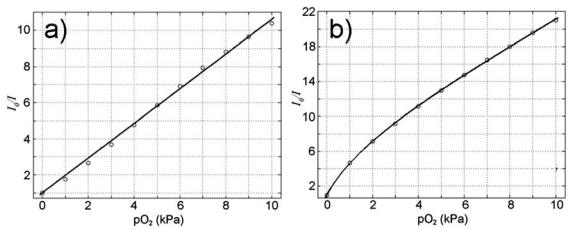

Fig. 3 Stern–Volmer plots in the range 0–10 kPa O_2 for (a) **1**-PS and (b) **1**-AP200/19 obtained by intensity measurements.

for the lifetime measurements.

Table 2 O_2 sensitivity of sensing films using luminescence intensity measurements and apparent luminescence lifetimes estimated from phase shift measurements

Range	Parameters	**1**-PS	**1**-AP200/19
Intensity measurements[a] (I_0/I)			
0–100 kPa pO_2	K_{SV1} (kPa^{-1})	1.628 ± 0. 132[b]	3.490 ± 0.107[b]
	x_1	0.94 ± 0.01	0.97 ± 0.01
	K_{SV2} (kPa^{-1})	0.00 ± 0.00	0.0515 ± 0.0064
	x_2	0.06 ± 0.01	0.03 ± 0.01
	R^2	0.9623 ± 0.0075	0.9999 ± 0.0006
0–10 kPa pO_2	K_{SV1} (kPa^{-1})	0.93 ± 0.07[c]	5.450 ± 0.323[b]
	x_1	1.0 ± 0.0	0.9 ± 0.1
	K_{SV2} (kPa^{-1})	—	0.200 ± 0.014
	x_2	—	0.09 ± 0.06
	R^2	0.9926 ± 0.0115	0.9966 ± ± 0.0084
Lifetime measurements[a] (τ_0/τ)			
0–10 kPa pO_2	K_{SV1} (kPa^{-1})	0.280 ± 0.040[b]	5.590 ± 0.160[b]
	x_1	0.76 ± 0.08	0.68 ± 0.09
	K_{SV2} (kPa^{-1})	0.010 ± 0.020	0.030 ± 0.070
	x_2	0.24 ± 0.09	0.31 ± 0.08
	R^2	0.9998 ± 0.0004	0.9988 ± 0.0009
0–1 kPa pO_2	K_{SV1} (kPa^{-1})	0.190 ± 0.010[b]	9.740 ± 0.870[b]
	x_1	0.62 ± 0.01	0.63 ± 0.09
	K_{SV2} (kPa^{-1})	0.200 ± 0.030	0.090 ± 0.050
	x_2	0.38 ± 0.02	0.37 ± 0.08
	R^2	0.9996 ± 0.0003	0.9998 ± 0.0002

[a] [Dye concentration] = 1.5 mg mL^{-1}; the results are the average of 3 replicas $\pm st/\sqrt{n}$ (n = 3, t = 4.303 ($2P$ = 0.05), s = standard deviation). [b] Data fitted with the Demas two-site model. [c] Data fitted with the Stern–Volmer model.

1-AP200/19 and **1**-PS, in Fig. S5 (ESI†) for **2**-AP200/19 and **2**-PS and in Fig. S6 (ESI†) for **3**-PS. The fitting parameters for films containing **1** are reported in Table 2 (see Table S2 for other films, ESI†). As anticipated, the use of the nanostructured support AP200/19 increased the oxygen sensitivity, as shown by the increase of the Stern–Volmer constant values. In particular **1**-AP200/19 sensitivity is more than 5 times the sensitivity of **1**-PS. Such sensitivity improvement has previously been observed for Pt(II), Ru(II), and Ir(III) oxygen sensitive dyes[5,7,17,18] and is now demonstrated for the first time with Cu(I) dyes, which confirms that the improvement is qualitatively due to the nanostructured film.

The most sensitive sensing films are based on **1**- and **2**-AP200/19 (K_{SV1} = 5.45 and 5.13 kPa^{-1}, respectively). Comparing these results with classical Pt(II), Ru(II), and Ir(III) sensing films using the same nanostructured matrix (see Table 1), it is clear that Cu(I) sensing films are very promising for O_2-sensing applications. Indeed, Ir(III) sensing films show lower sensitivity. Only PtTFPP shows higher sensitivity in the same condition (K_{SV} = 25.68 kPa^{-1}).[5]

Intensity measurements are not sensitive enough to characterize the sensing films in the range 0–1 kPa pO_2. Therefore we used a multifrequency phase-modulation method for luminescence spectroscopy using a rectangular-wave modulated excitation source with a short duty cycle[19] for measuring lifetime for this range of oxygen concentrations.§ It provides: (1) a more complete characterization of the luminescence system (multiple frequencies measured at once), and (2) an improvement in the accuracy for determining the analyte concentration.[19]

After finding the appropriate modulation frequency for each sensing film for best signal-to-noise ratio, 10% duty cycle

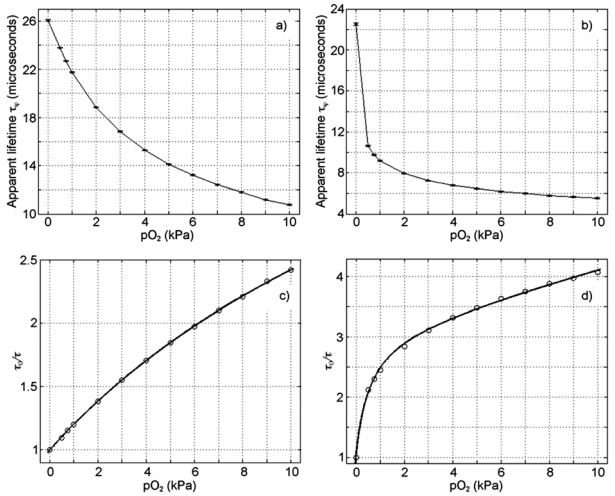

Fig. 4 Apparent lifetimes determined from the phase-shift (τ_φ in μs) of (a) **1**-PS and (b) **1**-AP200/19 at 21 °C in the range 0–10 kPa O_2; and Stern–Volmer plot of (c) **1**-PS and (d) **1**-AP200/19 fitted using the Demas two-site model.

rectangular-wave excitation signals with the selected modulation frequencies (*i.e.*, with fundamental frequencies of 5650 Hz and 14 125 Hz for **1**-PS and **1**-AP200/19 films, respectively, see ESI† for details) were used to carry out the calibration of the sensing films.[19]

Oxygen-sensitive properties of **1**-PS and **1**-AP200/19 were determined following the procedure described in ESI.† The calibration curves for **1**-PS and **1**-AP200/19 when exposed to different oxygen concentrations are shown in Fig. 4 and the results are summarized in Table 2. As for intensity measurements, the incorporation of the dye into AP200/19 increased the sensitivity of the film to oxygen. Gratifyingly, intensity and lifetime measurements provided similar results for high oxygen concentrations (K_{SV1} of **1**-AP200/19 by intensity is 5.45 kPa^{-1} and by lifetime is 5.59 kPa^{-1} for the range 0–10 kPa O_2). At low oxygen concentrations (range 0–1 kPa O_2) K_{SV1} of **1**-AP200/19 is 9.74 kPa^{-1}, demonstrating the high sensitivity of the film in these conditions.

To demonstrate that these new sensing films can also be used for ultra-low oxygen detection, we used synthetic air (mixture of oxygen and nitrogen) to achieve a minimum oxygen concentration of 0.05 kPa pO_2. The phase-based luminescence lifetime variations for different oxygen levels between 0 and 2.1 kPa pO_2 are shown in ESI† (see Fig. S9, ESI†). $\Delta\tau_{0.05}$ was used to characterize the sensitivity of the sensing films for concentrations over 0.05 kPa pO_2. This parameter was determined following the following equation:[5]

$$\Delta\tau_{0.05} = \frac{\tau_0 - \tau_{0.05}}{\tau_0 - \tau_{100}} \times 100$$

where τ_0 corresponds to the luminescence lifetime in the absence of oxygen, $\tau_{0.05}$ is the luminescence lifetime in the presence of 0.05 kPa (0.05%) oxygen and τ_{100} is the luminescence lifetime in the presence of 100 kPa (100%) oxygen. **1**-PS has $\Delta\tau_{0.05} = 1.50 \pm 0.32\%$ while **1**-AP200/19 shows a much higher $\Delta\tau_{0.05} = 33.55 \pm 0.37\%$. In practice it means that the 33.55% of the signal of the emission is quenched at 0.05 kPa pO_2. Comparing these results with previous works using the same methodology and same set-up (Table 1), we confidently conclude that **1**-AP200/19 is more sensitive at ultra-low O_2 concentrations than Ir(III) complexes (*i.e.* $\Delta\tau_{0.05}$ for N969, N1008 and EB146 immobilized in the same solid support and performing the measurements in the same conditions are 20.98 ± 1.02%, 4.44 ± 0.70% and 9.43 ± 1.41%, respectively). Among the noble metal-based sensing films, only PtTFPP-AP200/19 ($\Delta\tau_{0.05} = 62.53 \pm 3.66\%$) displays better performance, which is one of the most sensitive films at ultra-low O_2 concentration reported in the literature.

To demonstrate the practicality of these sensing films, the oxygen concentration of several air samples were measured with the films and compared with the real O_2 concentrations (Table S3, ESI†). Because of their higher sensitivity, films based on AP200/19 are more accurate with intensity methods, while both AP200/19 and PS have similar accuracy with lifetime measurements.

The quenching reaction does not consume oxygen and therefore the process is reversible as demonstrated by results shown in Fig. S4–S6 (ESI†). As the most relevant application for these sensing films is trace oxygen analysis, the response and recovery times have been calculated between 1 and 5 kPa pO_2, which provide more relevant information than response times to 100 kPa pO_2 and recovery to anoxic condition. The t_{95} response times for all of the sensing films are given in Table S4 (ESI†). All of them are shorter than 11 s when changing from 1 to 5 kPa pO_2 and shorter than 16 s when changing from 5 to 1 kPa pO_2. The registered response times are in fact the response times of the full system that is the time needed to change O_2 concentration from 1 to 5 kPa pO_2 and *vice versa*.

An important concern common to all optical sensors is the degradation of their quantum efficiency following prolonged sampling and continuous illumination. To evaluate the photostability of the sensing films, they were illuminated with a UV lamp (λ = 315 nm and 6 Watt power) during 6 h. The photostability study (Fig. 5 for **1**-PS and **1**-AP200/19 and Fig. S10, ESI† for other films) was carried out at 21 °C for three oxygen concentrations (0, 2, and 8 kPa). Data were collected every hour, using intensity measurements. The most stable sensing film was **2**-PS, which suffered the least degradation (12% of the signal after 6 hours).

Finally, the effect of humidity on the sensing response was assessed to further evaluate the applicability of the films. Five sensing films based on **1**-PS and **1**-AP200/19 were used to determine the concentration of oxygen between 0 and 20 kPa

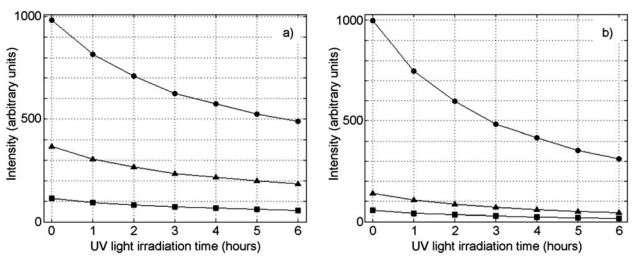

Fig. 5 Photostability of (a) **1**-PS and (b) **1**-AP200/19 at 21 °C for various oxygen concentrations using intensity measurements (● 0 kPa pO_2; ▲ 2 kPa pO_2; ■ 8 kPa pO_2).

at different levels of relative humidity (0, 10, 20, 40 and 80% RH) (Fig. S11, ESI†). **1**-PS was not affected by RH because of the hydrophobicity of PS. On the other hand, the sensitivity of **1**-AP200/19 decreased as the RH increased. It is due to the high hydrophilicity of this matrix, which had been previously pointed out.[7,20] Thus, **1**-AP200/19 is more useful for gaseous analysis and the relative humidity of the environment has to be taken into account during the calibration of the sensing film.

Three luminescent Cu(I)-complexes were investigated for the optical sensing of low and ultra-low oxygen concentrations using intensity and phase-based apparent lifetime measurements. The organometallic complexes were incorporated into a classical PS membrane and a nanostructured, metal oxide matrix AP200/19.

This is the first time that Cu(I) complexes have been incorporated into AP200/19. The spectral properties of these dyes are not affected by the solid support. The most sensitive sensing films are **1**-AP200/19 and **2**-AP200/19 (K_{SV1} = 5.45 and 5.13 kPa^{-1}, respectively, in the range 0–10 kPa pO_2). Interestingly they show higher sensitivity than reported sensing films based on phosphorescent cyclometallated Ir(III) complexes (*e.g.* K_{SV}(N969-AP200/19) = 4.79 kPa^{-1}) but still lower than PtTFPP complex (K_{SV}(PtTFPP-AP200/19) = 25.68 kPa^{-1}). As expected from the definition of K_{SV}, sensitivity is primarily better correlated to the lifetime of excited state of the emitting species than to the photoluminescent quantum yield of the film, which provides a direction of research to further increase the sensitivity of these promisingly low cost copper-based emitters.

Furthermore these sensing films are suitable for ultra-low oxygen detection down to 0.05 kPa pO_2. In particular the parameter $\Delta\tau_{0.05}$ (33.55 ± 0.37%) shows that **1**-AP200/19 is again more sensitive at ultra-low O_2 concentrations than films based on Ir(III) complexes and as much as the half of the most sensitive AP200/19-based sensing films at ultra-low O_2 concentration reported in the literature ($\Delta\tau_{0.05}$ for PtTFPP-AP200/19 is 62.53 ± 3.66%).

The reasons for the excellent performance of **1** are primarily attributed to the pertinent choice of matrix and measurement method. As other complexes are not as performing as **1**, specific properties of **1** are also important for high performance. However definitive conclusions about this aspect cannot be drawn because only **1** could be fully studied.

Overall, we have clearly demonstrated that copper-based luminescent complexes are a credible alternative to more expensive emitters for oxygen sensing and deserve particular attention for the development of low cost O_2 sensing films.

The authors gratefully acknowledge the financial support of the Spanish Ministry of Economy and Competitiveness (CTQ2011-25316 and Medina-Rodríguez's grant reference BES-2009-026919), the Regional Government of Andalusia (Excellence projects P07-FQM-2625 and P07-FQM-2738), and the European Union (MulTHIC, IEF-326107, and HetIridium, CIG-322280). Also, the authors are grateful to Ilford Imaging Switzerland GmbH (Switzerland) for supplying the metal oxide membranes.

Notes and references

‡ **3**-AP200/19 gave irreproducible O_2-sensing results and is not discussed further. This is attributed to its more hydrophobic nature compared to other dyes, resulting in significant aggregation in the highly polar AP200/19.

§ Only films using **1** were characterized using lifetime measurements in the frequency domain (phase-resolved method) because of the impossibility to excite other films with the 375 nm UV LED used in our set-up.

1 N. Armaroli, G. Accorsi, F. Cardinali and A. Listorti, *Top. Curr. Chem.*, 2007, **280**, 69.
2 (*a*) N. Alonso-Vante, J.-F. Nierengarten and J.-P. Sauvage, *J. Chem. Soc., Dalton Trans.*, 1994, 1649; (*b*) T. Bessho, E. C. Constable, M. Graetzel, A. H. Redondo, C. E. Housecroft, W. Kylberg, M. d. K. Nazeeruddin, M. Neuburger and S. Schaffner, *Chem. Commun.*, 2008, 3717; (*c*) Y.-J. Yuan, Z.-T. Yu, J.-Y. Zhang and Z.-G. Zou, *Dalton Trans.*, 2012, **41**, 9594; (*d*) T. E. Hewat, L. J. Yellowlees and N. Robertson, *Dalton Trans.*, 2014, **43**, 4127; (*e*) M. S. Lazorski and F. N. Castellano, *Polyhedron*, 2014, **82**, 57.
3 (*a*) J. C. Deaton, S. C. Switalski, D. Y. Kondakov, R. H. Young, T. D. Pawlik, D. J. Giesen, S. B. Harkins, A. J. M. Miller, S. F. Mickenberg and J. C. Peters, *J. Am. Chem. Soc.*, 2010, **132**, 9499; (*b*) M. Hashimoto, S. Igawa, M. Yashima, I. Kawata, M. Hoshino and M. Osawa, *J. Am. Chem. Soc.*, 2011, **133**, 10348; (*c*) F. Wei, T. Zhang, X. Liu, X. Li, N. Jiang, Z. Liu, Z. Bian, Y. Zhao, Z. Lu and C. Huang, *Org. Electron.*, 2014, **15**, 3292; (*d*) A. Wada, Q. Zhang, T. Yasuda, I. Takasu, S. Enomoto and C. Adachi, *Chem. Commun.*, 2012, **48**, 5340.
4 (*a*) N. Armaroli, G. Accorsi, M. Holler, O. Moudam, J. F. Nierengarten, Z. Zhou, R. T. Wegh and R. Welter, *Adv. Mater.*, 2006, **18**, 1313; (*b*) Q. S. Zhang, Q. G. Zhou, Y. X. Cheng, L. X. Wang, D. G. Ma, X. B. Jing and F. S. Wang, *Adv. Funct. Mater.*, 2006, **16**, 1203; (*c*) R. D. Costa, D. Tordera, E. Ortí, H. J. Bolink, J. Schonle, S. Graber, C. E. Housecroft, E. C. Constable and J. A. Zampese, *J. Mater. Chem.*, 2011, **21**, 16108.
5 S. Medina-Rodriguez, M. Marin-Suarez, J. F. Fernandez-Sanchez, A. de la Torre-Vega, E. Baranoff and A. Fernandez-Gutierrez, *Analyst*, 2013, **138**, 4607.
6 S. M. Borisov, P. Lehner and I. Klimant, *Anal. Chim. Acta*, 2011, **690**, 108.
7 J. F. Fernández-Sánchez, R. Cannas, S. Spichiger, R. Steiger and U. E. Spichiger-Keller, *Anal. Chim. Acta*, 2006, **566**, 271.
8 M. T. Miller and T. B. Karpishin, *Sens. Actuators, B*, 1999, **61**, 222.
9 L. Shi, B. Li, S. Yue and D. Fan, *Sens. Actuators, B*, 2009, **137**, 386.
10 C. S. Smith and K. R. Mann, *Chem. Mater.*, 2009, **21**, 5042.
11 Y. Wang, B. Li, Y. Liu, L. Zhang, Q. Zuo, L. Shi and Z. Su, *Chem. Commun.*, 2009, 5868.
12 C. S. Smith, C. W. Branham, B. J. Marquardt and K. R. Mann, *J. Am. Chem. Soc.*, 2010, **132**, 14079.
13 J. Yuasa, M. Dan and T. Kawai, *Dalton Trans.*, 2013, **42**, 16096.
14 C. S. Smith and K. R. Mann, *J. Am. Chem. Soc.*, 2012, **134**, 8786.
15 A. Kaeser, M. Mohankumar, J. Mohanraj, F. Monti, M. Holler, J.-J. Cid, O. Moudam, I. Nierengarten, L. Karmazin-Brelot, C. Duhayon, B. Delavaux-Nicot, N. Armaroli and J.-F. Nierengarten, *Inorg. Chem.*, 2013, **52**, 12140.
16 (*a*) C. S. Smith, C. W. Branham, B. J. Marquardt and K. R. Mann, *J. Am. Chem. Soc.*, 2010, **132**, 14079; (*b*) J. Yuasa, M. Dan and T. Kawai, *Dalton Trans.*, 2013, **42**, 16096; (*c*) R. Czerwieniec, K. Kowalski and H. Yersin, *Dalton Trans.*, 2013, **42**, 9826; (*d*) X.-L. Chen, R. Yu, Q.-K. Zhang, L.-J. Zhou, X.-Y. Wu, Q. Zhang and C.-Z. Lu, *Chem. Mater.*, 2013, **25**, 3910.
17 M. Marín-Suárez del Toro, J. F. Fernández-Sánchez, E. Baranoff, M. K. Nazeeruddin, M. Gräetzel and A. Fernández-Gutiérrez, *Talanta*, 2010, **82**, 620.
18 M. Marín-Suárez, B. F. E. Curchod, I. Tavernelli, U. Rothlisberger, R. Scopelliti, I. Jung, D. Di Censo, M. Grätzel, J. F. Fernández-Sánchez, A. Fernández-Gutiérrez, M. K. Nazeeruddin and E. Baranoff, *Chem. Mater.*, 2012, **24**, 2330.
19 S. Medina-Rodríguez, A. de la Torre-Vega, F. J. Sainz-Gonzalo, M. Marín-Suárez, C. Elosúa, F. J. Arregui, I. R. Matias, J. F. Fernández-Sánchez and A. Fernández-Gutiérrez, *Anal. Chem.*, 2014, **86**, 5245.
20 J. F. Fernández-Sánchez, I. Fernández, R. Steiger, R. Beer, R. Cannas and U. E. Spichiger-Keller, *Adv. Funct. Mater.*, 2007, **17**, 1188.